

PCCP

Accepted Manuscript



This article can be cited before page numbers have been issued, to do this please use: T. S. Sundar, R. Sen and P. Johari, *Phys. Chem. Chem. Phys.*, 2016, DOI: 10.1039/C6CP00367B.



This is an *Accepted Manuscript*, which has been through the Royal Society of Chemistry peer review process and has been accepted for publication.

Accepted Manuscripts are published online shortly after acceptance, before technical editing, formatting and proof reading. Using this free service, authors can make their results available to the community, in citable form, before we publish the edited article. We will replace this *Accepted Manuscript* with the edited and formatted *Advance Article* as soon as it is available.

You can find more information about *Accepted Manuscripts* in the [Information for Authors](#).

Please note that technical editing may introduce minor changes to the text and/or graphics, which may alter content. The journal's standard [Terms & Conditions](#) and the [Ethical guidelines](#) still apply. In no event shall the Royal Society of Chemistry be held responsible for any errors or omissions in this *Accepted Manuscript* or any consequences arising from the use of any information it contains.

Rationally Designed Donor-Acceptor Scheme based Molecules for Applications in Opto-Electronic Devices

T. Subash Sundar^{1,†}, R. Sen^{2,‡} and P. Johari^{2*,‡}

Department of Electrical Engineering, School of Engineering, Shiv Nadar University, NH91, Tehsil Dadri, Gautam Buddha Nagar, U. P.-201314. India, and Department of Physics, School of Natural Sciences, Shiv Nadar University, NH91, Tehsil Dadri, Gautam Buddha Nagar, U. P.-201314. India

E-mail: priya.johari@snu.edu.in, psony11@gmail.com

Abstract

Several donor(D)-acceptor(A) based molecules are rationally designed by adopting three different schemes in which conjugation length, strength of the donor and acceptor moieties, and planarity of the molecules are varied by introducing a π -conjugated linkage unit, terminating ends of the moieties by different electron donating and accepting functional groups, and fusing the donor and acceptor moieties, respectively. Our DFT and TDDFT based calculations reveal that using the abovementioned designing schemes, the electronic and optical properties of the D-A based molecules can be largely tuned. While introduction of linkage and fusing of moieties enhances the

*To whom correspondence should be addressed

[†]Department of Electrical Engineering, School of Engineering, Shiv Nadar University, NH91, Tehsil Dadri, Gautam Buddha Nagar, U. P.-201314. India

[‡]Department of Physics, School of Natural Sciences, Shiv Nadar University, NH91, Tehsil Dadri, Gautam Buddha Nagar, U. P.-201314. India

$\pi - \pi$ interaction, addition of electron donating groups (-CH₃, -OH, -NH₂) and electron accepting groups (-CF₃, -CN, -NO₂, -NH₃⁺) vary the strength of the donor and acceptor moieties. These factors lead to modulation in the HOMO and LUMO energy levels and facilitate engineering of the HOMO-LUMO gap and the optical gap over a wide range of $\sim 0.7 - 3.7$ eV. Moreover, on the basis of calculated ionization potential and reorganization energy, most of the investigated molecules are predicted to be air stable and to exhibit high electron mobility, with the possibility of presence of ambipolar characteristics in few of them. The results of our calculations not only demonstrate the examined molecules to be the potential materials for the organic opto-electronic devices, but also establishes an understanding on the composition-structure-property correlation which will prove as a guideline for designing and synthesizing new materials of choice.

KEYWORDS: Rational designing, Density functional theory, Electronic structure properties, Optical Properties, Organic molecules, Donor-Acceptor moieties

INTRODUCTION

The research on “Band Gap Engineering” has attracted an increasing amount of attention in recent years because it helps in tuning the properties of materials. This has encouraged numerous researchers to design novel organic molecules and polymers that can pose potential advantages over mainstream inorganic-based semiconductor devices by significantly reducing the material/fabrication cost, increasing flexibility and at the same time giving comparable efficiency and improved functionality. This gives organic molecules a potential to realize molecular electronics as the future of next-generation opto-electronic devices. In this work we aim to study donor (D)-acceptor (A) based organic molecules by performing *in silico* analysis to obtain their ground state geometry, electronic, and optical properties.

Interaction of donor moiety (D) possessing small ionization potential with an acceptor moiety (A) having large electron affinity, results in the reduction of the gap between the

energy levels of highest occupied molecular orbital (HOMO) and the lowest unoccupied molecular orbital (LUMO) with respect to the HOMO-LUMO energy gap of the individual molecular entity.¹⁻⁹ In past few years, several studies have been made to examine the D-A based molecules and polymers by choosing various types of donor and acceptor moieties under several schemes.⁴⁻¹³ These studies have successfully demonstrated the possibility to tune the properties of the molecular materials with the change in donor-acceptor moieties.^{5,8-12} However, these studies are limited and there is a need to explore these molecules to the full capacity. We, therefore, aim to investigate several rationally designed D-A based small organic molecules, modeled mainly using following three schemes:

- (a) Coupled D-A-A-D with linkage (L) configuration, *e.g.*, D-L-A-L-A-L-D,
- (b) Coupled D-A-D configuration with additional electron donor and accepting groups at the terminating ends,
- (c) Fused DA configuration with electron donor and accepting groups at the terminating ends.

A comparative study of molecules designed using above mentioned schemes is done to examine the effect of molecular structure and composition on the opto-electronic properties. This comparative study will help us to establish a correlation between chemical composition, structure and properties. All calculations are performed using ab-initio approach, based on density functional theory (DFT) and time-dependent DFT (TDDFT), in conjunction with generalized gradient approximation (GGA) based PBE and hybrid HSE06 exchange correlation (xc) functionals. Inclusion of a part of exact exchange ensures the superior quality and reliability of our HSE06 results. Our calculations show promising results. We found that the molecules designed by following the above mentioned schemes are capable of engineering the electronic and optical gap over a wide energy range, covering near infrared (IR)-to-visible-to-near ultraviolet (UV) region of the solar light. Thus, making these materials potential candidates for the applications in devices like OLEDs, OFETs, and OPVs. Moreover, an

understanding about the basic properties of these molecules will not only give us an opportunity to design more novel organic small molecules and copolymers with tunable optical and electronic gap but will also help us in observing the charge mobility, reorganization energy of the charges and their correlation with the properties of the Donor-Acceptor moieties. This will eventually provide a better understanding for rational designing of organic molecules and the science behind the band gap engineering and the charge transfer in organic copolymers, which pose a strong potential in shouldering the future of the organic electronics industry globally.

MOLECULAR STRUCTURES AND COMPUTATIONAL DETAILS

Structures

A series of D-A scheme based molecules are modeled considering aforementioned configurations. All investigated molecules contain thiophene as the donor moiety and benzo-thiadiazole or benzo-bis-thiadiazole as the acceptor moiety (see Figure 1). The D-A based molecules are in general terminated by long alkyl chains to increase their solubility in organic solvents. However, instead of considering long chains we have terminated the ends either by an electron donating group (EDG) or/and electron accepting group (EAG). We assume that replacing long alkyl chains by methyl group will not change our results in any significant way. While, use of EDG or EAG of various strengths may affect the results, which we intend to study. An EDG is a functional group that donates some of its electron density into a π -conjugated system *via* resonance. On the contrary, an EAG has the opposite effect as it removes electron density from a π -conjugated system, which should affect the overall strength of the moiety to which it is attached.

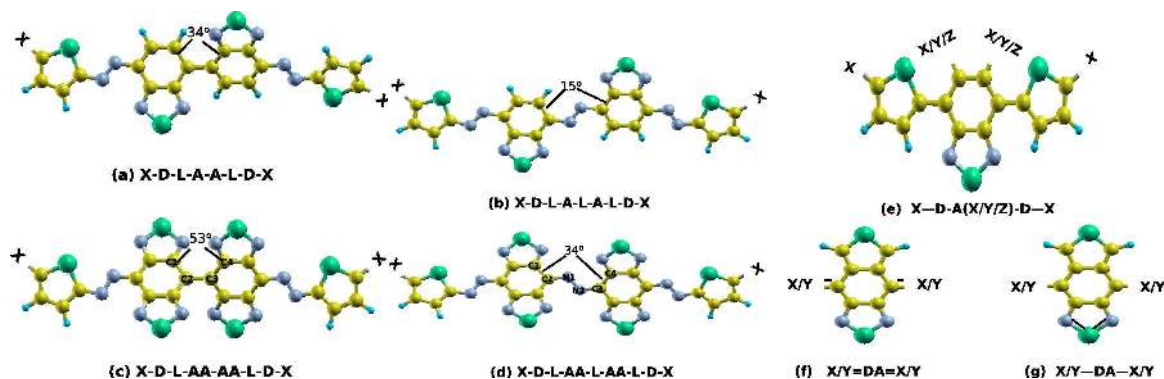


Figure 1: (a)–(d): D-A-A-D molecules with linkages (L) between D-A and A-A units for non-bis (a and b) and bis (c and d) configurations of acceptor moiety; (e): Coupled D-A-D molecules with donor and acceptor ends terminated by EDG (X) or/and EAG (Y) or/and Hydrogen (Z); (f): Fused DA molecule in A'-configuration (having double bonds at the terminating ends) and (g): in B'-configuration, having single bonds at the terminating ends. Fused molecules are also terminated by different EDGs or/and EAGs. EDGs (X) are chosen from $-\text{CH}_3$, $-\text{OH}$, and $-\text{NH}_2$ functional groups while either of the $-\text{CF}_3$, $-\text{CN}$, $-\text{NO}_2$, and $-\text{NH}_3^+$ is considered as EAG.

The first configuration of D-A based molecules is modeled using D-A-A-D molecule as the base molecule where 'D' denotes a thiophene unit which acts as donor moiety and 'A' denotes a benzo-thia-diazole or benzo-bis-thia-diazole (AA) unit which represents the acceptor moiety, and attaching π -conjugated linkage group between D-A and A-A units. For this, we coupled the donor and acceptor units as the $\text{NH}_2\text{-D-L-A-A-L-D-NH}_2/\text{NH}_2\text{-D-L-A-L-A-L-D-NH}_2$ molecules with azo ($-\text{N}=\text{N}-$) or ethylene ($-\text{CH}=\text{CH}-$) linkages (L or L1, respectively). Addition of linkage not only increases the conjugation length but can also reduce the torsion between the moieties and hence, increase the planarity of the molecule and also the $\pi-\pi$ interaction. We mostly considered D-A-A-D molecules terminated by a $-\text{NH}_2$ electron donating group, but to examine the effect of strength of EDG, few molecules with $-\text{CH}_3$ as terminating end groups are also studied. This arrangement gives us primarily following molecules to explore: $\text{EDG-D-(L/L1)-A-A-(L/L1)-D-EDG}$ and $\text{EDG-D-(L/L1)-A-(L/L1)-A-(L/L1)-D-EDG}$ with non-bis configuration (A) of acceptor moiety (Figure 1 (a) and (b)), and $\text{EDG-D-(L/L1)-AA-AA-(L/L1)-D-EDG}$ and $\text{EDG-D-(L/L1)-AA-(L/L1)-AA-(L/L1)-D-EDG}$ with bis configuration (AA) of acceptor moiety (Figure 1 (c) and (d)).

In second category, the coupled D-A-D molecules are chosen mainly to examine the effect of strength of donor and acceptor moieties on the opto-electronic properties. For this purpose, various EDGs and EAGs are attached to the terminating ends of the donor or/and acceptor moieties, to vary their strength. We considered EDGs as $-\text{CH}_3$, $-\text{OH}$, and $-\text{NH}_2$ groups (X) and EAGs as $-\text{CN}$, $-\text{NO}_2$, and NH_3^+ groups (Y). A model of this type of molecules is presented in Figure 1 (e).

The third configuration of molecules are the fused DA molecules that are modeled with the idea to increase the planarity in the molecule. By fusing the donor and acceptor moieties we induce the rigidity in the backbone of the molecule, that enhances the planarity, which should lead to reduction in the HOMO-LUMO energy gap. Thus, in our fused DA configuration based molecules, a thiophene ring is fused with the benzene ring of the acceptor moiety, *i.e.*, benzo-thiadiazole having B'(A') configuration, and the ends are terminated by electron donating groups (EDG/X) like: $-\text{NH}_2$ ($=\text{NH}$), $-\text{CH}_3$ ($=\text{CH}_2$), or $-\text{OH}$, or/and by electron accepting groups (EAG/Y) such as: $-\text{CF}_3$ ($=\text{CF}_2$), $-\text{NH}_3^+$, $-\text{NO}_2$, $-\text{CN}$ as shown in Figure 1 (f) and (g), to vary the strength of donor and acceptor moieties. The functional group with single bond will lead to the B'-configuration of the acceptor moiety, while the groups with double bond will constitute the A'-configuration.

Structural Relaxation and Electronic Properties

Electronic and ionic relaxations are performed using ab-initio DFT based approach as implemented in the Vienna Ab-Initio Simulation (VASP) Package.^{14,15} The electron-ion interactions are treated using projector-augmented-wave (PAW) potentials.¹⁶ While, to account exchange correlation effects, hybrid exchange-correlation (xc) functional, Heyd-Scuseria-Ernzerhof (HSE06), is considered.¹⁷⁻²⁰ It is though well known that the semi-local functional (GGA) in DFT underestimate the band gap, while hybrid functionals that have a certain percentage of Hartree-Fock (HF) exchange generally lead to better agreement with experiments. But, for the sake of comparison with TDDFT calculations which are quite

expensive with HSE06 functional for large molecules and beyond the scope of current work, relaxation of some of the molecules is also performed using semi-local GGA functional in PBE (Perdew–Burke–Ernzerhof) flavor.²¹ All the calculations are done with a plane wave cutoff of 400 eV and single \mathbf{k} -point, *i.e.*, the Γ -point. Atomic relaxation is performed until the interatomic forces are less than 0.01 eV/Å, which is found sufficient to obtain the relaxed geometry. In order to realize the molecule by avoiding any interaction between the translational images, a vacuum region of around 12 Å is adopted along all three directions.

It is well acknowledged that in semiconducting organic materials, at room temperature, the charge transport phenomenon can be explained by the diffusion process in which the charge carrier hops from one molecule to the neighboring molecule.^{22,23} Thus, charge carrier mobility mainly depends on two factors: the reorganization energy λ and the coupling matrix element V . The reorganization energy defines the energy due to (i) structural reorganization because of addition or removal of a charge carrier and (ii) changes in the surrounding medium (solvent) because of polarization effects. In current scenerio we neglect the latter contribution as we are not considering the materials in solution phase and calculate λ_h and λ_e , only due to structural modification of material on the addition of a hole and an electron, respectively. Since, in the molecular crystal the contribution from polarization of neighboring molecules is significantly small, the calculations for λ are performed by considering the neutral and the charged configurations of the materials in the molecular phase. Figure 2 depicts a schematic diagram for calculations of λ . It shows three potential surfaces corresponding to neutral and charged molecule. The structure of each molecule in neutral and charged (cation and anion) configurations are relaxed until atomic forces are less than 0.01 eV/Å. Afterwards, using four energies corresponding to: (i) optimized geometry of neutral molecule, E_0 , (ii) neutral configuration of optimized charged geometry, E_+^0/E_-^0 , (iii) optimized geometry of charged molecule, E_+/E_- , and (iv) charged (cation/anion) configuration of optimized neutral geometry, E_0^+/E_0^- , the reorganization energy due to addition of a hole and electron are computed as:

$$\lambda_h = \lambda_{1h} + \lambda_{2h} = (E_+^0 - E_0) + (E_0^+ - E_+). \quad (1)$$

$$\lambda_e = \lambda_{1e} + \lambda_{2e} = (E_-^0 - E_0) + (E_0^- - E_-). \quad (2)$$

The ionization potential (IP), electron affinity (EA), and fundamental electronic gap (E_{fund}) corresponding to all molecules are calculated using expressions:

$$IP = E_0 - E_0^+ , \quad (3)$$

$$EA = E_0^- - E_0 , \quad (4)$$

$$E_{fund} = IP - EA . \quad (5)$$

Optical Properties

To demonstrate the absorption capability of examined molecules in the visible region of the solar spectra we studied the linear absorption spectra of corresponding molecules using TDDFT suite available in the Quantum Espresso (QE) code.²⁴⁻²⁶ All simulations are performed within TDDFT^{27,28} with plane wave basis set, by adopting norm-conserving pseudo-potentials. Both, semi-local GGA functional in PBE flavor and hybrid functional in HSE06 flavor are used to calculate the absorption spectra, depending on the size of the molecule. Calculations are done considering a planewave cutoff of 80 Ry and single \mathbf{k} -points, *i.e.*, the Γ -point. To compute the absorption spectra, we used turboTDDFT components of QE, in which Davidson-like approach is implemented to find out the solution of Casida's equation in spectral representation. Since, we are only interested in illustrating the low-lying absorp-

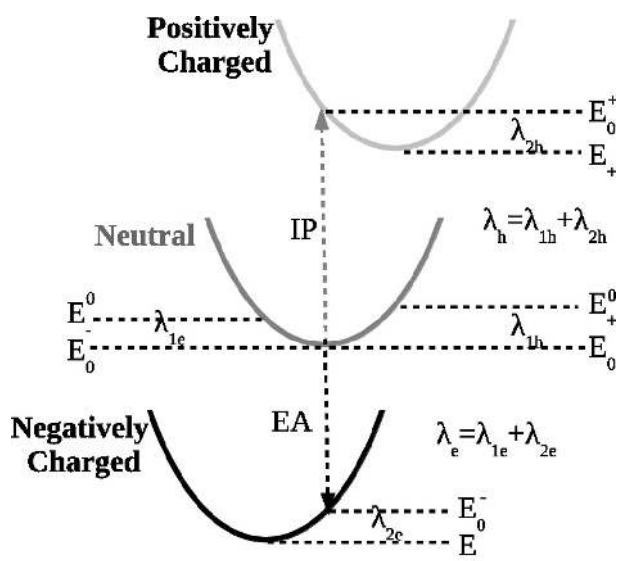


Figure 2: Schematic representation of the potential energy surfaces of neutral and charged molecules. The reorganization energy for hole and electron is calculated as: $\lambda_h = \lambda_{1h} + \lambda_{2h}$ and $\lambda_e = \lambda_{1e} + \lambda_{2e}$, respectively, where λ_1/λ_2 represents the energy difference between neutral/charged configurations of neutral and charged molecules. Energies corresponding to neutral and charge geometries are represented by subscript '0' and '+/−', respectively. Energies related to optimized geometry are shown without a superscript, while the charged (+/−) and neutral (0) configurations are represented with their respective symbols as superscript. Ionization potential (IP) is calculated as $E_0^+ - E_0$ and electron affinity (EA) is calculated as $E_0 - E_0^-$.

tion spectra of the examined molecules, Davidson-like approach in TDDFT, is much more appropriate as it deals only with few eigen triplets of Liouvillian matrix in the restricted energy region of the spectra.²⁶ It is also less expansive in the perspective of computational time with respect to Liouvillian-Lanczos method in TDDFT,²⁵ which is quite appealing for the whole excitation spectra. For turboDavidson calculations, 30 Liouvillian-eigen triplets are computed for all cases, with estimated error in the eigenvalues to be below 10^{-4} Ry. We further restricted ourselves by choosing the energy region in the linear absorption spectra, stating from 0 Ry to 0.5 Ry in the step of 0.0002 Ry. The computed spectra has been broadened by calculating them at complex frequencies $\omega + i\eta$, with $\eta = 0.005$ Ry. Note that similar to TDDFT, the QE code could also be used for DFT calculations, which would not make any significant quantitative or qualitative difference in our current results. However, we preferred to use VASP for the DFT calculations as the base molecules of two of the considered configurations (D-A-A-D and D-A-D) are taken from our previous work,²⁹ which used VASP for structure relaxation.

RESULTS AND DISCUSSIONS

The key factors that play major role in defining the HOMO-LUMO energy gap or the optical gap in a D-A based organic molecule are: (i) conjugation length, (ii) planarity of the molecule, and (iii) strength of the donor and acceptor moieties. Therefore, in the present work, molecules are rationally designed keeping one or more of these factors in mind. As discussed, the molecules are designed under three different schemes. We will discuss their structural, electronic, and optical properties one by one.

D-A-A-D Molecules with Linkage:

In one of our recent paper²⁹ we have shown a large torsion to exist in between A-A units of thiophene benzo-chalogen-diazole molecules. This torsion particularly attains a huge value

(dihedral angle $> 50^\circ$) in case of molecules having acceptor units as benzo-bis-chalcogen-diazole, which in turn disrupt the conjugation length and increase the gap between HOMO and LUMO energy levels. However, to design an efficient organic opto-electronic device, especially an OPV or OFET, we need materials with longer conjugation length and lower HOMO-LUMO gap. Therefore, here we put an effort to reduce the torsion between A-A units of the D-A-A-D molecule by introducing a linkage unit between them, in order to increase its conjugation length and decrease the HOMO-LUMO energy gap. Table 1 presents the difference between Kohn-Sham HOMO and LUMO energy levels, ΔE^{KS} , computed using PBE and HSE06 xc functional for the pristine D-A-A-D molecules and the D-A-A-D molecules with linkage (-N₂- or -(CH)₂-). It is well known that in case of organic molecules, the difference between HOMO-LUMO energy levels calculated using DFT within HSE06 framework generally gives a good approximation to the optical gap, while PBE flavor of xc functional, underestimates it.²⁹⁻³¹ To prove this, a comparative study between DFT computed ΔE^{KS} and TDDFT calculated optical gap (E_{opt}) would be ideal. However, performing TDDFT calculations using HSE06 potential for the molecules with linkage are beyond the scope of current work. We, therefore, calculated low-lying absorption spectra using TDDFT approach with PBE xc-functional, which may still underestimates the optical gap but will give a qualitative estimation of the absorption spectrum and the optical gap. The TDDFT computed optical gap using PBE xc-functional is given in parenthesis in Table 1. The molecular length, difference between ionization potential (IP) and electron affinity (EA), E_{fund} , that defines the fundamental gap for the molecule, together with their hole and electron reorganization energies, λ_h and λ_e , are also tabulated in Table 1.

It is evident from Table 1 that the Kohn-Sham energy gap (HOMO-LUMO energy gap) decreases consistently with the addition of linkage between the moieties. The addition of linkage between D and A units increases the molecular length and thus, the conjugation length (see HOMO in Figure 3), which results into decrease in the gap between HOMO and LUMO energy levels by ~ 0.2 eV, as compared to molecules without linkage. The linkage

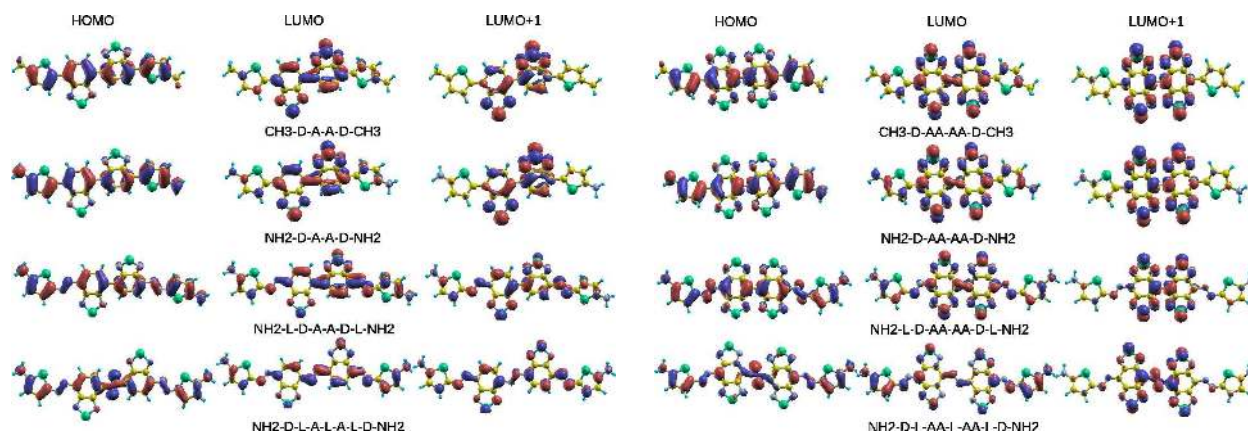


Figure 3: Left hand figure shows the *HOMO*, *LUMO*, and *LUMO* + 1 orbitals of EDG-D-A-A-D-EDG molecules with and without linkages (-N=N-) between D-A and A-A moieties with non-bis configuration. Right hand figure depicts the same for the bis configuration (AA) of acceptor moiety. The isosurface are drawn at the value of $0.001 \text{ eV}/\text{\AA}^3$. To examine the effect of strength of donor moiety, different EDGs such as, -CH₃ and -NH₂ are used.

between D and A units negligibly affect the torsion between them, as the dihedral angle between D and A unit remains to a value $\sim 5^\circ$.²⁹ While, the addition of linkage between A-A/AA-AA units not only further increases the length, but also reduces the steric hindrance between them and lowers the torsion angle to roughly half ($\sim 15^\circ/34^\circ$) in comparison to the torsion between A-A/AA-AA units without linkage ($\sim 34^\circ/53^\circ$).²⁹ This additionally leads to decrease in the HOMO-LUMO energy gap by roughly 0.3 – 0.6 eV. Both azo (L) and ethylene (L1) linkages reduce the gap in similar fashion. This suggests that the π -conjugated linkage group works as a bridge for covalent polarization that enhances the $\pi - \pi$ interaction.¹¹ Moreover, this is also evident from Figure 4 which represents the PDOS of selected carbon/nitrogen atoms (that describes the torsion between acceptor units) of NH₂-D-L-AA-AA-L-D-NH₂ and NH₂-D-L-AA-L-AA-L-D-NH₂ molecules that the steric hindrance between the A-A units decreases. From the insets of the figure it is clear that there is negligible overlapping between the p_x - p_x orbitals in case of prior molecule, while it increases substantially in the latter case. The increased contribution of p_x -orbitals in NH₂-D-L-AA-L-AA-L-D-NH₂ molecule justifies the reduction in the dihedral angle due to addition of linkage units.

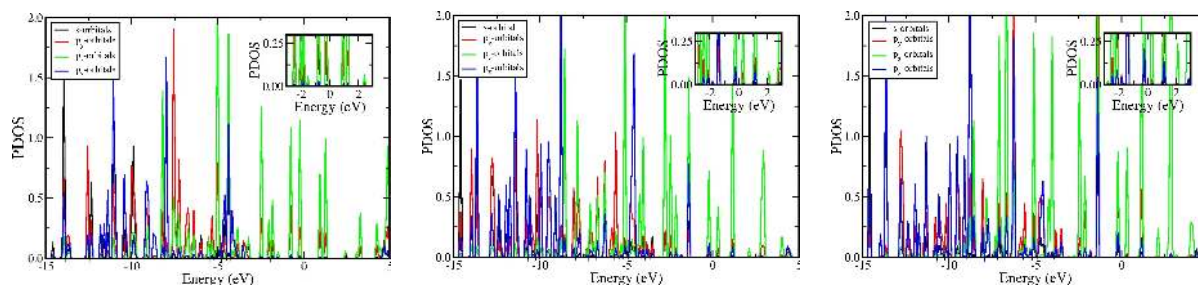


Figure 4: Left hand side graph depicts the PDOS of carbon atoms (C1-C2-C3-C4) connecting the acceptor units and describing the torsion between the acceptor units in the $\text{NH}_2\text{-D-L-AA-AA-L-D-NH}_2$ molecule, while middle and right hand side graphs depict the PDOS of (C1-C2-C3-C4) and (C2-N1-N2-C3) atoms, respectively, in the $\text{NH}_2\text{-D-L-AA-L-AA-L-D-NH}_2$ molecule (see Figure 1). Insets show the enlarged graph in a short energy range between $-3 - 3$ eV.

On comparing the effect of non-bis (A) and bis (AA) configuration of acceptor moieties, we found that similar to previous study, ΔE^{KS} of the bis-molecules is smaller as compared to the respective molecules with non-bis configuration.²⁹ Capping the ends of the molecule by different electron donating groups (EDGs), $-\text{CH}_3$ and $-\text{NH}_2$, also seems to reasonably affect the HOMO-LUMO energy levels and the gap between them. A difference of approximately 0.2 eV is noticed between the HOMO-LUMO energy gap of D-(L)-A-A-(L)-D molecules, capped with $-\text{CH}_3$ or $-\text{NH}_2$ electron donating groups. The strong electron donating strength of $-\text{NH}_2$ than $-\text{CH}_3$ results into 0.2 eV lower HOMO-LUMO gap in case of molecules capped with $-\text{NH}_2$. Thus, by linking donor and acceptor units with a linkage like azo or ethylene group and considering a stronger EDG as the terminal groups, the gap between the HOMO-LUMO energy levels can widely be tuned from ~ 2.2 eV to 1.0 eV (Table 1), which covers near infra-red to the yellow light region of the solar spectrum.

Table 1 tabulates the ΔE^{KS} calculated using HSE06 (PBE) xc-functionals. On comparing the results for $\text{CH}_3\text{-D-A-A-D-CH}_3$ with the available experimental data for the electrochemical and optical band gap,¹ it is found that PBE largely underestimates while HSE06 computed value of 2.22 eV gives good agreement with the experimental value of ~ 2.2 eV, which warrants the correctness of our approach. On this basis, we assume HSE06 to predict the optical gap accurately for other investigated molecules as well, since it is well known that

HSE06 computed Kohn-Sham gap agrees well with the optical gap of organic molecules.^{30,31} A comparison with TDDFT results would however be useful but studying optical absorption spectra using TDDFT with HSE06 xc-functional was not feasible with the available computational resources, therefore, we have calculated the TDDFT spectra of the considered D-A-A-D molecules (with and without linkage) using PBE functional. From Figure 5, it is clearly evident that introduction of linkage between A-A (or AA-AA) units lowers the optical gap and red shifts the absorption spectra. Also, a red shift in the spectrum of $\text{NH}_2\text{-D-A(AA)-A(AA)-D-NH}_2$ as compared to spectrum of $\text{CH}_3\text{-D-A(AA)-A(AA)-D-CH}_3$ can easily be observed, as the effect of strong EDG at the terminating ends. The first peak of the spectrum of $\text{NH}_2\text{-D-A(AA)-A(AA)-D-NH}_2$ corresponds mainly to $|HOMO \rightarrow LUMO\rangle$ transition along the long molecular axis, while in molecules with linkages ($\text{NH}_2\text{-D-L-A(AA)-A(AA)-L-D-NH}_2$, $\text{NH}_2\text{-D-L-A(AA)-L-A(AA)-L-D-NH}_2$), the first peak is found due to almost equivalent weightage from $|HOMO \rightarrow LUMO\rangle$, $|HOMO \rightarrow LUMO + 1\rangle$ and $|HOMO - 3 \rightarrow LUMO\rangle$ transitions. The *HOMO* is localized mainly on donor and linkage, while *LUMO* and *LUMO + 1* are nearly localized on acceptor in case of molecules without linkage. In molecules with linkages *LUMO* and *LUMO + 1* are localized on acceptor, as well as on linkages (Figure 3). Thus, in molecules with linkages, transition from donor to linkage, linkage to linkage or linkage to acceptor also seems to play important role. This states that the linkage groups not only facilitate the planarization of the molecules but also contribute to the intramolecular charge transfer, which can lead to better light harvesting in the photovoltaic devices.^{11,12} Also, it is noticed that with increasing number of linkages, the features in the absorption spectrum also increase, which further reflects the contribution of linkage group in the intramolecular transition. These features correspond to a band of transitions from several lower occupied states to *LUMO* and from *HOMO* to various higher occupied states. On comparing the molecules with bis and non-bis configuration of acceptor units, we found a decrease in energy in the spectrum of bis-molecules, as compared to non-bis ones, similar to the HOMO-LUMO energy gap.

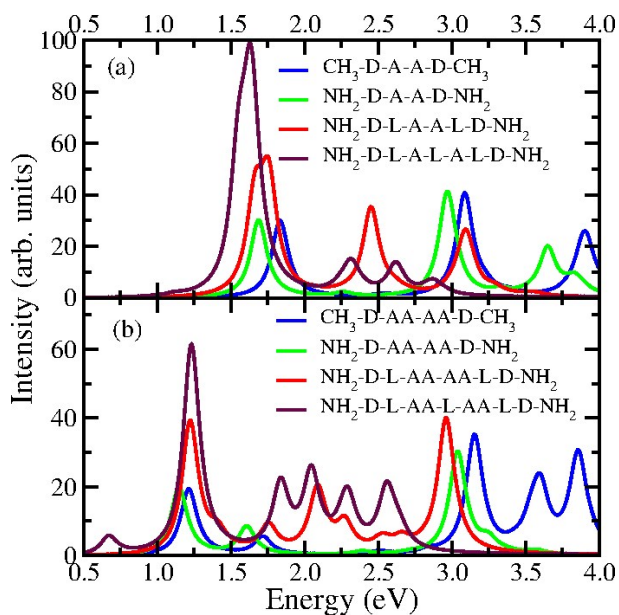


Figure 5: Low-lying absorption spectra of various (top) EDG-D-A-A-D-EDG and (bottom) EDG-D-AA-AA-D-EDG molecules (having non-bis and bis configuration, respectively), with and without linkage (azo) between D-A and A-A units. Two different EDGs: $-\text{CH}_3$ and $-\text{NH}_2$, are considered to examine the effect of strength of donor moiety. All spectra are calculated using TDDFT approach with PBE xc-functional.

On analyzing fundamental gap from Table 1, we found that the fundamental gap also decreases with the addition of linkage between the moieties. Similar to Koopmans' theorem in the closed-shell Hartree-Fock theory, in DFT, the vertical ionization potential (IP) and vertical electron affinity (EA) can directly be related to the HOMO and LUMO energy levels, respectively. The difference between IP and EA gives the fundamental gap (E_{fund}). However, DFT provides only an approximation to the IP and EA, thus the fundamental gap and the quality of this approximation very much depends on the nature of the xc-functional. A disagreement in the computed and measured values of IP, EA, and E_{fund} is therefore foreseen. Since, most of the molecules under investigation are the rationally designed, the experimental values of optical and fundamental gaps are not available at the moment. Therefore, we can not directly compare our results with the experiments. However, on comparing calculated data with the measured data available for $\text{CH}_3\text{-D-A-A-D-CH}_3$ we found calculated IP of 5.13 eV to be in good agreement with the experimental value of

5.50 eV. A small difference can be anticipated due to different alkyl chains considered in experiments and our calculations. The IP of all examined D-A-A-D based molecules lie in the range of 4.2 – 5.5 eV. Since IP can directly be related to the HOMO energy level, looking at the energy range one can predict that these low lying HOMO levels will be useful for better air stability and open-circuit voltages of photovoltaic devices.^{11,12} A large difference is seen in the value of EA, where computed EA (1.98 eV) is overestimated by roughly 1 eV from the measured value (~ 3.3 eV). This difference is in agreement with the results obtained by Polander *et al.*³ for benzothiadiazole-dithienopyrrole based D-A-D molecules. Experimentally, the fundamental gap or the electrochemical gap is estimated from the difference between oxidation and reduction potentials, and optical gap is obtained from the onset of absorption in solution. Quite often, they come close to each other giving a negligible exciton binding energy ($E_B = E_{fund} - E_{opt}$).^{1,3} This is because the effects of exciton binding are effectively compensated for by solvation of the ions formed in the electrochemical experiments. This gives an ambiguity in the measured electrochemical gap and thus, the difference between the measured and the calculated fundamental gap is obvious. For all investigated molecules in current series we found the exciton binding energy to be between 0.7 – 0.9 eV, which is well under the range described for exciton binding energies in organic semiconductors.³² It is also seen that the exciton binding energy decreases with the increase in the molecular length, which is attributed to the delocalization of carriers over the length of the molecule.³³

On analysing reorganization energy, we found the reorganization energy for electrons (λ_e) to be lesser than that for holes (λ_h). Both λ_e and λ_h are found to increase with the addition of linkage, stating more structural changes on addition or removal of an electron due to presence of linkage unit. The λ_e further decreases in bis configuration as compared to non-bis configuration. The value of λ_e varies between $\sim 0.12 - 0.33$ eV, while λ_h varies from $\sim 0.27 - 0.48$ eV. Mostly, it is observed that lower value of reorganization energy leads to better charge carrier mobility.^{34,35} Thus, we predict a higher electron mobility than the

hole mobility for D-A-A-D molecules with linkage. On this hypothesis, we assume that the electron mobility can be improved by considering a weaker EDG, *i.e.*, -CH₃, bis configuration of benzo-thia-diazole acceptor moiety, and ethylene linkage over the stronger EDG as -NH₂, non-bis configuration of the acceptor moiety and azo linkage, respectively.

D-A-D Molecules with various EDGs and EAGs:

Next we investigate the coupled D-A-D based molecules with different electron donating and accepting groups attached to the donor and acceptor moieties. The idea of adding these groups is to examine the effect of variation in the strength of donor and acceptor moieties due to additional electron donating or/and accepting functional groups, on the opto-electronic properties. In principle, the increase in the strength of donor or acceptor moieties should decrease the HOMO-LUMO energy gap.²⁹ However, how efficiently these functional groups will help in tuning the opto-electronic properties of D-A-D based molecules is not well studied. Therefore, in present work, we used various electron donating groups (EDGs) such as: -CH₃, -NH₂, and -OH, and electron accepting groups (EAGs) like -CN, -NO₂, and -NH₃⁺, with smallest thiophene benzo-thia-diazole based D-A-D molecule as the central unit (Figure 1(e)). This study will also help in characterizing the strength of these electron donating and accepting functional groups.

It is well known that -OH and -NH₂ donate electrons and -CN and -NO₂ withdraw electrons via. resonance effect, while -CH₃ and -NH₃⁺ groups donate and accept electrons, respectively, due to inductive effect. On examining Table 2, we find that the addition of EDG or/and EAG substantially affects the HOMO-LUMO energy gap. Attaching an EDG to the donor moiety (D=thiophene) increases the over all strength of the donor moiety by donating electrons to the thiophene ring *via.* resonance (-R) or induction (+I) effect. This results into reduction in the HOMO and LUMO energy levels and they move towards zero energy as per the strength of the EDG. The destabilization of HOMOs is found to be more as compared to LUMOs on going from -CH₃ to -OH to -NH₂ (see Table 2), which leads to a

Table 1: Energy levels corresponding to HOMO (E_{HOMO}) and LUMO (E_{LUMO}) and respective Kohn Sham HOMO-LUMO energy gap ($\Delta E^{KS} = E_{HOMO} - E_{LUMO}$) calculated using HSE06 (PBE) xc-functional for D-A-A-D molecules, with and without azo (-N₂-) or ethylene -(CH)₂- linkage between the D-A and A-A moieties, are given. For comparison, TDDFT computed optical gap using PBE xc-functional, is also presented in parenthesis. Ionization potential (IP), electron affinity (EA), fundamental gap ($E_{fund} = IP - EA$), together with hole and electron reorganization energies (λ_h and λ_e) are also tabulated. These quantities are calculated using HSE06 xc-functional.

Molecule	a (Å)	E_{HOMO} (eV)	E_{LUMO} (eV)	ΔE^{KS} (eV)	E_{opt} (eV)	IP (eV)	EA (eV)	E_{fund} (eV)	λ_e (eV)	λ_h (eV)
D-A-A-D Molecules with Linkage										
CH ₃ -D-A-A-D-CH ₃	15.08	-4.72	-2.50	2.22 (1.47)	(1.83)	5.13	1.98	3.15	0.19	0.29
NH ₂ -D-A-A-D-NH ₂	15.07	-4.22	-2.25	1.97 (1.24)	(1.69)	4.61	1.76	2.85	0.24	0.47
CH ₃ -D-N ₂ -A-A-N ₂ -D-CH ₃	18.82	-5.14	-3.14	2.00 (1.25)	(1.45)	5.55	2.69	2.86	0.26	0.32
NH ₂ -D-N ₂ -A-A-N ₂ -D-NH ₂	18.80	-4.62	-2.82	1.79 (1.11)	(1.58)	5.01	2.41	2.60	0.29	0.46
NH ₂ -D-N ₂ -A-N ₂ -A-N ₂ -D-NH ₂	20.49	-4.57	-3.09	1.48 (0.84)	(1.11)	4.97	2.70	2.27	0.33	0.47
NH ₂ -D-(CH) ₂ -A-A-(CH) ₂ -D-NH ₂	19.71	-4.29	-2.52	1.77 (1.10)	(1.65)	4.70	2.02	2.68	0.21	0.42
NH ₂ -D-(CH) ₂ -A-(CH) ₂ -A-(CH) ₂ -D-NH ₂	21.81	-4.15	-2.54	1.61 (0.97)	(1.55)	4.53	2.11	2.43	0.17	0.39
CH ₃ -D-AA-AA-D-CH ₃	15.23	-4.44	-3.07	1.37 (0.82)	(1.09)	5.00	2.70	2.29	0.12	0.30
NH ₂ -D-AA-AA-D-NH ₂	15.20	-4.04	-2.87	1.17 (0.70)	(1.00)	4.46	2.43	2.03	0.19	0.46
NH ₂ -D-N ₂ -AA-AA-N ₂ -D-NH ₂	18.73	-4.24	-3.07	1.17 (0.66)	(1.12)	4.63	2.69	1.94	0.23	0.49
NH ₂ -D-N ₂ -AA-N ₂ -AA-N ₂ -D-NH ₂	20.66	-4.04	-3.49	0.55 (0.38)	(0.69)	4.42	3.16	1.26	0.21	0.48
NH ₂ -D-(CH) ₂ -AA-AA-(CH) ₂ -D-NH ₂	19.65	-4.01	-2.89	1.12 (0.66)	(1.04)	4.41	2.48	1.93	0.13	0.47
NH ₂ -D-(CH) ₂ -AA-(CH) ₂ -AA-(CH) ₂ -D-NH ₂	21.94	-3.87	-3.17	0.70 (0.38)	(0.93)	4.19	2.77	1.42	0.14	0.37

decrease in the HOMO-LUMO energy gap in the similar fashion. Considerably larger HOMO densities than LUMO densities and the increase in HOMO densities on going from $-\text{CH}_3$ to $-\text{OH}$ to $-\text{NH}_2$ also reflect the destabilization of HOMOs¹³ through introduction of EDGs of various strengths (see Figure 6). It is noticed that addition of EDGs to the donor moiety does not make any significant change to the molecular base. The molecule remains planar as they were without EDGs. Also, it is well known that $-\text{CH}_3$ is a weakly activating (+I) group, while $-\text{OH}$ and $-\text{NH}_2$ are amongst strongly activating (-R) group. Our calculations, however, further characterize these groups and arrange them in order of increasing strength as: $-\text{CH}_3 < -\text{OH} < -\text{NH}_2$.

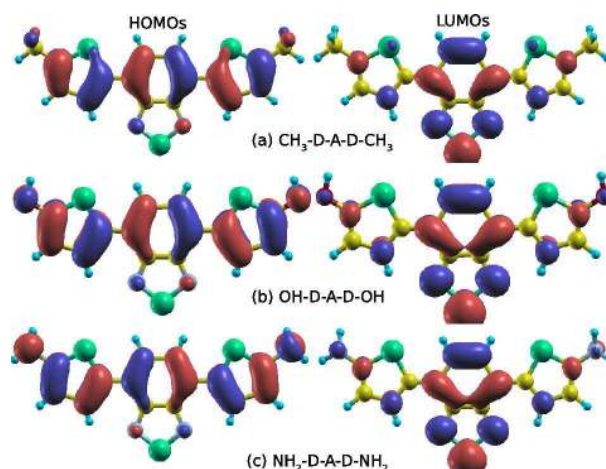


Figure 6: HOMOs and LUMOs of EDG-D-A-D-EDG molecules. EDGs are taken as $-\text{CH}_3$, $-\text{OH}$, and $-\text{NH}_2$ groups.

Keeping the EDG connected to the donor moiety, on substituting H by EDG in the acceptor unit ($A = \text{benzo-thia-diazole}$), the strength of the acceptor moiety decreases in general as by donating electrons to the benzo-thia-diazole, EDG weakens the electron affinity of the acceptor moiety. Moreover, addition of EDGs at the site of acceptor moiety also induces torsion between donor and acceptor moieties (dihedral angle between D-A units changes from $\sim 0^\circ$ to $\sim 30^\circ$), which results into reduction of conjugation length. Both of these effects lead to increase in the HOMO-LUMO energy gap. The LUMO energy level reduces substantially, while relatively much smaller change occurs in the HOMO energy level (see Table 2).

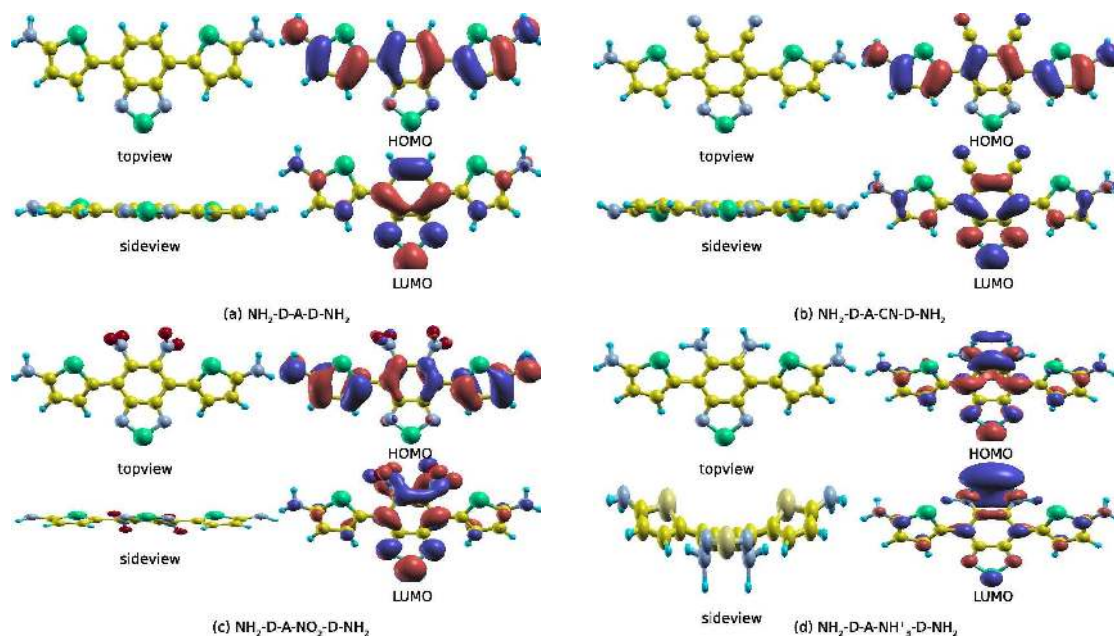


Figure 7: Topview and sideview of $\text{NH}_2\text{-D-A-(H/EAG)-D-NH}_2$ molecules, with $\text{EAG} = \text{-CN}$, -NO_2 , and -NH_3^+ groups. HOMOs and LUMOs of respective molecules are also given along their side.

However, instead of EDGs, if EAGs replace the H atoms connected to the benzene ring of benzo-thia-diazole acceptor moiety, the overall strength of the acceptor moiety increases due to +R or -I effect. This also leads to destabilization of the HOMO and LUMO energy levels but, through increase in energy levels of both the orbitals with respect to the same molecule without EAG (with H atoms). However, here the increase in the LUMO energy level is relatively more prominent than the HOMO energy level. This further results into reduction of the HOMO-LUMO energy gap, ΔE^{KS} . Though, in this case the variation in the HOMO-LUMO energy gap is not in perfect synchronization with the strength of EAG. As known, -NH_3^+ is one of the strongest deactivating (-I) group, while -NO_2 and -CN fall under the category of strong deactivating (+R) groups with prior group stronger than the latter. Following this, the HOMO-LUMO energy gap should be in order as $\text{EDG-D-A-(CN)-D-EDG} > \text{EDG-D-A-(NO}_2\text{)-D-EDG} > \text{EDG-D-A-(NH}_3^+\text{)-D-EDG}$, while we found the HOMO-LUMO gap of these three molecules to be 1.78/1.97 eV, 1.94/2.21 eV, and 0.70/0.73 eV, respectively, when $\text{-NH}_2/\text{-OH}$ is considered as EDG. Thus, on the contrary to the above-

mentioned hypothesis, we obtained HOMO-LUMO energy gap of EDG-D-A-(NO₂)-D-EDG > EDG-D-A-(CN)-D-EDG. This contradiction arises from the fact that being a less strong group, introduction of -CN to the benzo-thia-diazole unit does not affect the basic structure of the molecule and the molecule remains mostly planar, while -NO₂, which implicates a stronger +R effect as compared to -CN, induces steric hindrance and thus a torsion angle of ~ 25° between the donor and acceptor moieties. This increase in the torsion between the D-A moieties in case of -NO₂ group as compared to -CN group, reduces the relative conjugation length and increases the HOMO-LUMO energy gap in the prior case than the latter. The EDG-D-A-(NH₃⁺)-D-EDG molecule though follows the expected trend but possesses an exceptionally low HOMO-LUMO energy gap, with quite low HOMO-LUMO energy levels (see Table 2). This can be explained by the strong -I effect of the -NH₃⁺ group which leads to polarization of the molecule by displacing the electron cloud in σ -bond towards the more electronegative N atoms of the -NH₃⁺ group as compared to C atoms of benzo-thia-diazole unit, making the molecule ionic in nature. An interesting fact is also seen on examining the structure of the EDG-D-A-(NH₃⁺)-D-EDG molecule. The introduction of -NH₃⁺ group to the acceptor moiety results into bending of the molecule in a saddle-shaped structure (see Figure 7). Thus both of these effects, the polarization of molecule and the saddle shape of the molecule, are assumed to be reason behind the low HOMO-LUMO energy gap in case of EDG-D-A-(NH₃⁺)-D-EDG molecule. This is also in agreement with the example of Coronene (a planar molecule) and Circulene (a saddle-shaped molecule), where the HOMO-LUMO energy gap of latter molecule is lesser than the former molecule.³⁶

Overall, our study reveals that by introducing electron donating or accepting groups of varying strength, the HOMO and LUMO energy levels can be tuned. This facilitates the band-gap engineering of D-A-D molecules over a wide energy range. For the examined EDG-D-A(H/EDG/EAG)-D-EDG molecules, we found the HOMO-LUMO energy gap to vary approximately in the range of 0.7 eV – 2.8 eV. By considering the molecule (NH₂-D-A(NH₃⁺)-D-NH₂) with strongest EDG and EAG attached to the donor and acceptor units,

respectively, the smallest HOMO-LUMO energy gap of 0.7 eV can be achieved, while by choosing the molecule (OH-D-A(NH₂)-D-OH) having strong EDG attached to both types of moieties a higher HOMO-LUMO energy gap of 2.8 eV can be obtained. Considering an EDG and EAG of relatively moderate strength will help in achieving the HOMO-LUMO energy gap in between the two extremes. The tunability of HOMO-LUMO gap covering near infra-red and the visible light range, makes these molecules promising for OLEDs and OPVs.

The optical properties of these molecules also follow similar trends and show that the optical gap can also be tuned over a wide energy range by considering different combinations of EDG and EAG at the terminating ends, as justified by our TDDFT calculations. On comparing ΔE^{KS} and E_{opt} from Table 2, it is evident that our DFT computed HOMO-LUMO energy gap matches well with the optical gap computed using TDDFT approach, with HSE06 xc-functional. An exception is however seen in case of ionic-type molecules having EAG as cationic -NH₃⁺ group. Since, the -NH₃⁺ group with strongest -I effect polarizes the molecule, we assume this small disagreement between HSE06 computed DFT and TDDFT values is due to inability of the TDDFT code to treat highly polarized molecules properly. The low-lying optical absorption spectra of EDG-D-A(H/EDG/EAG)-D-EDG molecules are presented in Figure 8. It is clear from Figure 8 (a) and (b) that quantitatively spectra drawn using PBE xc-functional are red shifted as compared to respective spectra calculated using HSE06, however, qualitatively both the functionals give similar spectra. We, therefore, will discuss the spectra plotted using PBE xc-functional, which qualitatively capture the essential features of the absorption spectrum. It is evident from the graphs presented in Figure 8 that mostly the optical gap decreases and the spectrum shifts towards lower energy range with the increase in the strength of donor and acceptor moieties due to addition of EDG and EAG, respectively. This happens because in general, for all molecules the first peak of the spectra corresponds to the $|HOMO \rightarrow LUMO\rangle$ transition and since introduction of EDG and EAG destabilize the HOMO and LUMO energy levels and cause a variation in the gap

between them as discussed earlier, the optical gap gets tuned as per the strength of EDG and EAG. The optical gap computed using HSE06 (PBE) xc-functional decreases on increasing the strength of donor moiety due to addition of electron donating $-\text{CH}_3$, $-\text{OH}$, and $-\text{NH}_2$ groups as 2.30 (2.00), 2.14 (1.82), and 1.95 (1.68) eV, respectively. Similarly, on increasing the strength of acceptor moiety through EAGs like $-\text{CN}$, $-\text{NO}_2$, and $-\text{NH}_3^+$ and keeping the EDG fixed as $-\text{NH}_2$, the optical gap decreases as 2.01 (1.50), 1.97 (1.53), and 0.87 (0.86) eV, respectively. Relatively large variation or the low optical gap in case of $\text{NH}_2\text{-D-A}(\text{NH}_3^+)\text{-D-NH}_2$ molecule can be understood by analyzing the HOMOs and LUMOs of molecules presented in Figure 7. It is evident that in $\text{NH}_2\text{-D-A}(\text{NH}_3^+)\text{-D-NH}_2$ molecule, HOMO mainly localizes over the benzo-thia-diazole while LUMO localizes over the $-\text{NH}_3^+$ group. Thus, the $|HOMO \rightarrow LUMO\rangle$ transition occurs between the benzo-thia-diazole unit and the $-\text{NH}_3^+$ group, i.e., transition occurs within the electron accepting entities. While, in all other molecules, the $|HOMO \rightarrow LUMO\rangle$ transition occurs between donor and acceptor units.

A deeper analysis of wavefunctions reveal that except in molecules having EAG as $-\text{NH}_3^+$, the first peak in spectra of all EDG-D-A(H/EDG/EAG)-D-EDG molecules originates mainly due the $|HOMO \rightarrow LUMO\rangle$ transition, but with small contribution from transitions $|HOMO \rightarrow LUMO + 1\rangle$ and $|HOMO \rightarrow LUMO + 2\rangle$. While, in $\text{NH}_2\text{-D-A}(\text{NH}_3^+)\text{-D-NH}_2$ and $\text{OH-D-A}(\text{NH}_3^+)\text{-D-OH}$ molecules the first peak is solely governed by $|HOMO \rightarrow LUMO\rangle$ transition. The second peak, which is mainly a prominent feature of all the spectra, originates majorly due to $|HOMO \rightarrow LUMO + 1\rangle$ transition in the molecules having only EDG, while in molecules having acceptor moiety terminated by a EAG, the major contribution comes from $|HOMO \rightarrow LUMO + 2\rangle$ or $|HOMO \rightarrow LUMO + 3\rangle$ transition.

No particular trend is noticed in IP and EA with respect to different EDG and EAG, however, they change such that the exciton binding energy ($E_B = E_{fund} - E_{opt}$) remains ~ 1.5 eV for most of the molecules. In $\text{NH}_2\text{-D-A}(\text{NH}_3^+)\text{-D-NH}_2$ molecule, however, strong EDG connected to donor moiety and strong EAG attached to the acceptor moiety leads to a smaller E_B of ~ 1.2 eV, while a weaker EDG and EAG connected to donor and acceptor

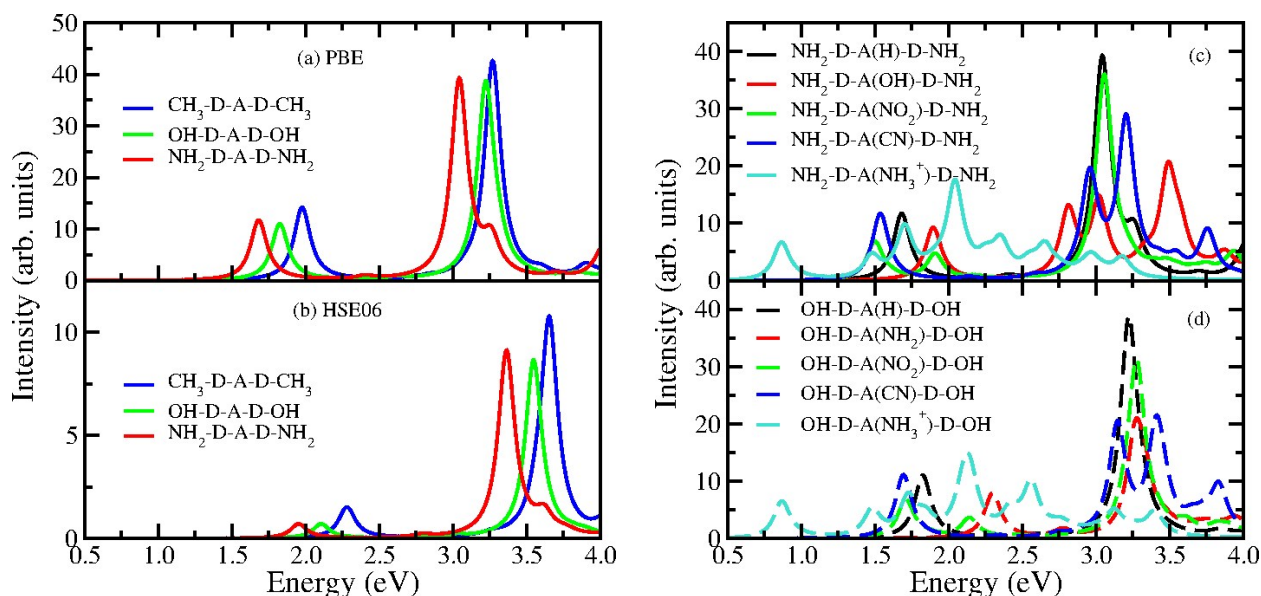


Figure 8: Left: Low-lying absorption spectra of various EDG-D-A-D-EDG molecules calculated using (a) PBE and (b) HSE06 xc-functionals. Right: Low-lying absorption spectra of (c) $\text{NH}_2\text{-D-A(EDG/EAG/H)-D-NH}_2$ and (d) $\text{OH-D-A(EDG/EAG/H)-D-OH}$ molecules, computed using PBE xc-functional. Three different EDGs: $-\text{CH}_3$, $-\text{OH}$, and $-\text{NH}_2$ and EAGs: $-\text{NO}_2$, $-\text{CN}$, $-\text{NH}_3^+$ are considered to examine the effect of strength of donor and acceptor groups, respectively. All spectra are calculated using TDDFT approach.

moieties, respectively, in $\text{OH-D-A(NO}_2\text{)-D-OH}$, results into a higher $E_B \sim 1.7$ eV. It is evident from Table 2 that the IP of most of these molecules lies between 5.0 – 6.0 eV, which is close to the work function of metals like Au, Pd, and Pt. This makes these materials air stable and potential candidates for devices like OFFTs and OPVs. The IP of molecules having $-\text{NH}_3^+$ group attached to the acceptor moiety do not lie in the range of 5.0 – 6.0 eV, but fall much below, at around 3.2 – 3.6 eV. Low IP in case of $\text{NH}_2\text{-D-A(NH}_3^+\text{)-D-NH}_2$ and $\text{OH-D-A(NH}_3^+\text{)-D-OH}$ molecules is not favourable, as the electrode material with matching work function will not be air-stable. Thus, though having a small electronic and optical gap, $\text{EDG-D-A(NH}_3^+\text{)-D-EDG}$ molecules will not be useful for device purpose.

On examining reorganization energy presented in Table 2, we noticed that in general λ_e is lower than λ_h for all investigated D-A-D based molecules, regardless of attached EDG and EAG. This suggests less variation in the molecular structure due to addition of electron as compared to hole. While, in particular, both λ_e and λ_h decreases with the increase in

strength of donor and acceptor moiety due to additional EDG and EAG, respectively. Thus, by considering different combinations of EDG and EAG with varying strength as terminating groups in D-A-D molecules, λ_e in the range $\sim 0.10 - 0.34$ eV and $\lambda_h \sim 0.33 - 0.57$ eV can be obtained. The lower value of λ_e than λ_h suggests a higher electron mobility for EDG-D-A(EAG)-D-EDG molecules,³⁵ which can further be improved by considering a longer molecule with more donor/acceptor units.

Fused DA Molecules:

The last set of investigated molecules are the fused D-A based molecules, in which donor and acceptor moieties are fused together to constitute a rigid molecule. Rigidity in molecular backbone is one of the prominent factor in tuning the opto-electronic properties of organic molecules, as the enhanced stiffness or planarity results in lowering the HOMO-LUMO energy gap. We therefore, instead of coupling (as in previous two schemes), fused together a thiophene and a benzo-thia-diazole moiety, and considered this smallest possible molecular unit as a prototype for our rationally designed fused DA molecules. The acceptor moiety, benzo-thia-diazole, is considered in two configurations having A' (=N-S-N=) and B' (-N=S=N-) groups, where in former case the terminating ends of benzene ring exhibit double bonds, while in latter case, the ends carry single bonds (Figure 1 (f) and (g), respectively). The benzene ring of the fused unit is terminated by various EDG or/and EAG, in order to examine the effect of these groups in tuning the properties of such rigid molecules.

On comparing the energy levels of the coupled D-A-D molecule (NH₂-D-A-D-NH₂) with fused DA molecule (NH₂-DA-NH₂) from Tables 2 and 3, we notice a decrease in the HOMO energy level (moving towards zero) while increase in the LUMO energy level (moving away from zero energy) of the latter molecule, with respect to the former. This results into a lower HOMO-LUMO energy gap of fused NH₂-DA-NH₂ molecule as compared to coupled NH₂-D-A-D-NH₂ molecule. Interestingly, the length of the coupled molecule is larger than the considered fused molecule but due to rigidity of the fused molecule there is enhanced

Table 2: Energy levels corresponding to HOMO (E_{HOMO}) and LUMO (E_{LUMO}) and respective Kohn-Sham HOMO-LUMO energy gap (ΔE^{KS}) calculated using HSE06 xc-functional, for the coupled D-A-D molecules with additional electron donating group (EDG: $-\text{CH}_3$, $-\text{OH}$, $-\text{NH}_2$) or/and electron accepting group (EAG: $-\text{NO}_2$, $-\text{CN}$, $-\text{NH}_3^+$) attached to the terminating ends, is given. For comparison, TDDFT computed optical gap using HSE06 (PBE) xc-functional, is also presented. Ionization potential (IP), electron affinity (EA), fundamental gap ($E_{fund}=\text{IP}-\text{EA}$), together with hole and electron reorganization energies (λ_h and λ_e) are also tabulated. These quantities are calculated using HSE06 xc-functional.

Molecule	a (Å)	E_{HOMO} (eV)	E_{LUMO} (eV)	ΔE^{KS} (eV)	E_{opt} (eV)	I.P. (eV)	E.A. (eV)	E_{fund} (eV)	λ_e (eV)	λ_h (eV)
D-A-D Molecules										
$\text{CH}_3\text{-D-A-D-CH}_3$	10.60	-4.99	-2.68	2.31	2.30 (2.00)	5.34	1.72	3.61	0.18	0.30
OH-D-A-D-OH	10.57	-4.72	-2.57	2.16	2.14 (1.82)	5.54	1.65	3.88	0.16	0.37
$\text{NH}_2\text{-D-A-D-NH}_2$	10.59	-4.33	-2.35	1.98	1.95 (1.68)	5.02	1.48	3.54	0.14	0.54
$\text{NH}_2\text{-D-A(OH)-D-NH}_2$	10.72	-4.23	-1.95	2.28	2.38 (1.89)	5.03	1.26	3.76	0.17	0.57
$\text{OH-D-A(NH}_2\text{)-D-OH}$	10.68	-4.70	-1.89	2.81	2.86 (2.30)	5.48	1.18	4.29	0.17	0.50
$\text{NH}_2\text{-D-A(CN)-D-NH}_2$	10.80	-4.63	-2.86	1.78	1.97 (1.53)	5.36	2.02	3.34	0.21	0.45
$\text{NH}_2\text{-D-A(NO}_2\text{)-D-NH}_2$	10.78	-4.78	-2.84	1.94	2.01 (1.50)	5.52	2.00	3.52	0.34	0.56
$\text{NH}_2\text{-D-A(NH}_3^+\text{)-D-NH}_2$	10.52	-2.57	-1.87	0.70	0.87 (0.86)	3.25	1.34	1.91	0.09	0.33
OH-D-A(CN)-D-OH	10.77	-5.18	-3.21	1.97	2.15 (1.69)	5.95	2.32	3.63	0.16	0.35
$\text{OH-D-A(NO}_2\text{)-D-OH}$	10.74	-5.28	-3.07	2.21	2.24 (1.71)	6.07	2.17	3.90	0.33	0.44
$\text{OH-D-A(NH}_3^+\text{)-D-OH}$	10.45	-2.86	-2.13	0.73	1.08 (0.86)	3.61	1.44	2.17	0.10	0.37

overlapping between π -orbitals of donor and acceptor moiety, which leads to reduction in the HOMO-LUMO energy gap.

Since the central unit of all fused molecules remains same, the length of the molecules does not vary much. Thus, the major difference in between the considered fused molecules comes from their terminating end groups, due to the type of the group (EDG or/and EAG) and the way they are attached to the central unit. The fused molecules in which the end groups are attached *via.* double bonds (*i.e.*, benzo-thia-diazole possesses =N-S-N= configuration) exhibit higher HOMO-LUMO energy gap than the fused molecules in which terminating groups are attached *via.* single bond (*i.e.*, benzo-thia-diazole possesses -N=S=N- configuration), due to reduced conjugation length in the case of former (Table 3 and Figure 9). The HOMO-LUMO energy gap lies in the near ultraviolet (UV) range between $\sim 3.5 - 4.1$ eV for the molecules having A'-configuration, while in the molecules with B'-configuration the transition between HOMO to LUMO energy level occurs at around $1.4 - 2.1$ eV, covering near infrared and red light region. Thus, even the smallest fused D-A based molecule in B'-configuration can be used for the red LEDs, and in A'-configuration it can be used for the application in near UV range, however, molecules will be less stable in latter composition due to connection of end groups *via.* less stable double bond as compared to the former case in which end groups are connected *via.* single bond.

The effect of EDG or EAG or mixture of that at the terminating ends of benzene ring of the fused molecule is also evident from the Table 3. The molecules having EDG exhibit lower HOMO-LUMO energy gap as compared to molecules with EAG. The hybrid configuration, *i.e.*, one end capped by EDG and the other end by EAG, possesses the gap in between. For example, $\text{NH}_2\text{-DA-NH}_2$ molecule having EDG as terminating group exhibits ΔE^{KS} of 1.43 eV and ΔE^{KS} for $\text{CF}_3\text{-DA-CF}_3$ molecule having EAG as terminating group is found to be 2.06 eV, while in case of $\text{NH}_2\text{-DA-CF}_3$ molecule, the ΔE^{KS} is obtained as 1.89 eV using HSE06 xc functional, which is in between the prior two values. On analyzing the trends in the HOMO-LUMO energy gap of molecules with different EDGs, we found that due to

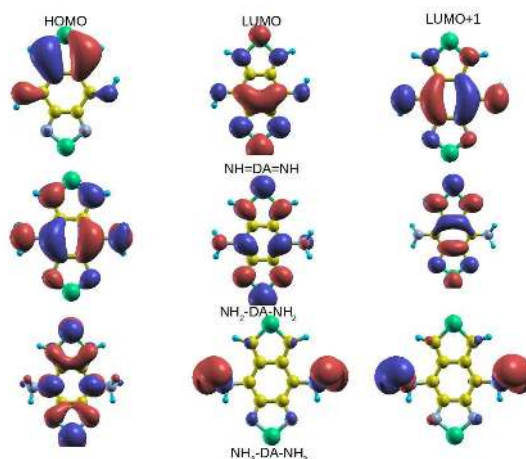


Figure 9: The *HOMO*, *LUMO*, and *LUMO* + 1 orbitals of fused DA molecules like: $\text{NH}=\text{DA}=\text{NH}$, $\text{NH}_2\text{-DA-NH}_2$, and $\text{NH}_3^+\text{-DA-NH}_3^+$. The first molecule has acceptor moiety in its A' -configuration, while last two have it in B' -configuration. Here, NH_2 and NH_3^+ groups act as the strong EDG and EAG, respectively. The isosurface are drawn at the value of $0.001 \text{ eV}/\text{\AA}^3$.

stronger resonance (-R) effect in molecules having -OH and - NH_2 groups, the HOMO and LUMO energy levels destabilize and move towards lower energy side with respect to $\text{CH}_3\text{-DA-CH}_3$. This effect is more pronounced in case of $\text{NH}_2\text{-DA-NH}_2$ molecule as compared to OH-DA-OH molecule, indicating - NH_2 group to be a stronger EDG than -OH group. This effect of the strength of the EDG clearly affects the HOMO-LUMO energy gap and the gap reduces with the increase in the strength of the electron donating group. Thereby, similar to the coupled EDG-D-A-D-EDG molecules, fused DA molecules also categorize the strength of EDGs in the order $-\text{CH}_3 < -\text{OH} < -\text{NH}_2$. Not so prominent, but similar trend of reduction in the HOMO-LUMO gap is observed in EAG-DA-EAG molecules, as well, indicating increasing strength of the electron accepting groups as: $-\text{CF}_3 < -\text{CN} < -\text{NO}_2 < -\text{NH}_3^+$, stating CF_3 to be a weaker EAG while NH_3^+ to be the strongest EAG. The - CF_3 , -CN, and - NO_2 groups accept electrons through resonance process (+R), while - NH_3^+ withdraws electrons *via*. induction effect (-I), which has much stronger effect by virtue of its positive charge that polarizes the molecule, and leads to exceptionally low HOMO-LUMO energy levels in case of $\text{NH}_3^+\text{-DA-NH}_3^+$ molecule, as compared to molecules with other EAGs. On the contrary, the HOMO and LUMO energy levels in the molecules with EAGs as - CF_3 or -CN or - NO_2 increases with

the increase in strength of the EAG. However, in general, the HOMO-LUMO energy gap reduces with the increase in the strength of EDG or EAG. The variation is more distinct in case of addition of EDG, as EDG increases the overall strength of the donor moiety by donating some of its electron density to the benzene ring, while addition of EAG results into reduction in the strength as EAG withdraws some of the electron density from the benzene ring, to which it is attached.

The optical gap (E_{opt}) calculated using TDDFT methodology in the framework of HSE06 xc-functional gives very good agreement with the DFT computed HOMO-LUMO energy gap using the same functional, while, as usual, PBE gives a smaller E_{opt} , as shown in Table 3. A sizable difference in DFT and TDDFT results is, however, noticed in case of molecule capped by $-\text{NH}_3^+$ EAG, but we attribute this to the incapability of considered TDDFT code to treat highly polarized molecules properly, similar to the case of coupled D-A-D molecules with $-\text{NH}_3^+$ group. It is well known that in DFT there is no unique xc-functional which can describe properties of all materials with same accuracy. Generally HSE06 is found to give good agreement with experiments³¹ but it is always desirable to have a one-to-one comparison with the experimental results. Since our rationally designed fused DA molecules are yet not explored experimentally, experiments are desired to clear the ambiguity about the difference.

Analyzing the spectra depicted in Figure 10, we noticed that the spectrum of molecules terminated by EDG have several low-intensity peaks within the range of 4 eV while the spectra of fused DA molecules terminated by EAG are blue shifted as compared to the spectra of molecules with EDG, exhibiting only two peaks within the given energy range. This is in coherence with the results obtained for HOMO-LUMO energy gap of these materials. In both cases, the first peak predominantly corresponds to the $|HOMO \rightarrow LUMO\rangle$ transition, while second peak occurs majorly due to $|HOMO \rightarrow LUMO + 1\rangle$ transition. The most intense peak for such molecules are obtained at higher energy (> 4 eV) which is mostly not captured in the spectra presented in Figure 10. Since, our aim was to obtain the optical

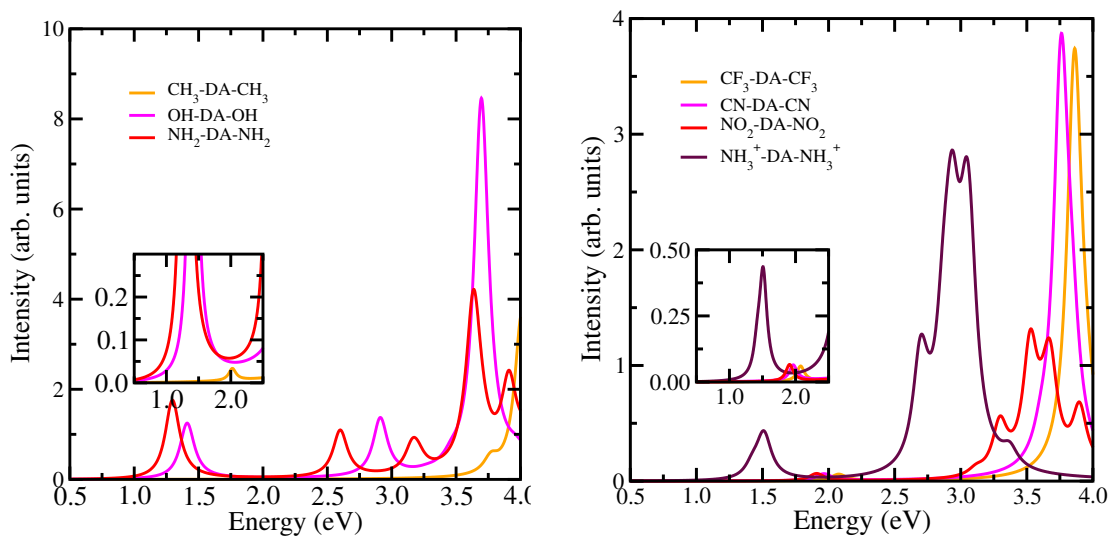


Figure 10: Low-lying absorption spectra of various EDG-DA-EDG (left) and EAG-DA-EAG (right) molecules whose general sketch is shown in Figure 1 (g). Various EDGs as $-\text{CH}_3$, $-\text{OH}$, and $-\text{NH}_2$ and EAGs like $-\text{CF}_3$, NO_2 , $-\text{CN}$, and NH_3^+ are used as terminating groups to vary the strength of the donor and acceptor moiety. Inset is showing the spectra zoomed in the energy region between 0.5 – 2.5 eV. All spectra are calculated using TDDFT approach with HSE06 xc-functional.

gap, we therefore, have focused mainly on the low energy range of the spectra. The optical spectrum for molecules with A'-configuration (in which end groups are connected *via*. double bond) are not presented here to avoid confusion, however, on comparing optical gap from the Table 3, it is evident that optical gap of molecules with A'-configuration is much higher than the molecules with B'-configuration. The higher optical gap is attributed to lower conjugation length in the former case as compared to latter (Figure 9). Although, similar to B'-configuration, in molecules with A'-configuration the first peak of the optical spectrum arises due to $|HOMO \rightarrow LUMO\rangle$ transition.

To further understand the respective transitions and also to understand the exceptional behavior of $\text{NH}_3^+-\text{DA}-\text{NH}_3^+$ molecule, we closely examined the isosurface plot of *HOMO*, *LUMO*, and *LUMO*+1 orbitals of three fused DA molecules ($\text{NH}=\text{DA}=\text{NH}$, $\text{NH}_2-\text{DA}-\text{NH}_2$, and $\text{NH}_3^+-\text{DA}-\text{NH}_3^+$) that represent different categories of fused molecules considered in this work. It is clear from the Figure 9 that *HOMO* is mainly localized over donor moiety and EDG, and *LUMO* and *LUMO* + 1 are mostly localized over the acceptor moiety or the

main molecular unit in NH=DA=NH and NH₂-DA-NH₂ molecules. While in NH₃⁺-DA-NH₃⁺ molecule, *HOMO* is localized over the main molecular unit, and *LUMO* and *LUMO* + 1 are localized completely on EAG. This elucidates transition of electrons from donor moiety or EDG to the acceptor moiety in the first two cases while reveals the transition of electrons from the main molecular unit to the -NH₃⁺ group and not to the acceptor moiety, in the third case. This explains the different behaviour of the molecules having -NH₃⁺ group.

On comparing IP of all investigated fused DA molecules from Table 3 we noticed that in molecules with B²-configuration IP mostly decreases/increases with the increase in the strength of EDG/EAG, while a contrary situation is seen in case of molecules having A¹-configuration. This happens due to shifting of HOMO energy level in an opposite manner. Most of the molecules, except OH-DA-OH and NH₂-DA-NH₂, are found to have high IP (> 6 eV) which does not match with the work function of the commonly used electrode materials. Thus, it may be difficult to use these materials for device application in their present form. Although, a bigger fused molecule may help to lower the IP and make these fused molecules useful for the application in opto-electronic devices.^{11–13} Trends similar to IP are witnessed in case of EA, as well. These materials exhibit EA in the wide range of ~1–3 eV, while the exciton binding energy ($E_B = E_{fund} - E_{opt}$) varies in the range of ~1.0–2.5 eV. In NH₃⁺-DA-NH₃⁺ molecule, a smaller E_B of ~ 1.0 eV is obtained, while at the same time the binding energy of other molecules having EDG or EAG is roughly ≥ 2 eV. The exceptionally low binding energy of NH₃⁺-DA-NH₃⁺ molecule is attributed to its ionic character.

On examining reorganization energy presented in Table 3, we noticed no particular trend with respect to EAG, however, on comparing for EDG we found that electronic reorganization energy tends to decrease with the increase in the strength of the electron accepting group, while hole reorganization energy sets an opposite trend. Altogether, the reorganization energy due to electron and hole varies over a wide range between ~ 0.04 – 0.30 eV and ~ 0.0–0.5 eV, respectively. Unlike D-A-D and D-A-A-D based materials which are predicted to have dominating electron charge mobility, we predict these materials to have either a high

electron (when terminated by EDG) or hole mobility (when terminated by EAG) or may also have ambipolar charge characteristics, depending on the choice and combination of electron donating and accepting groups.

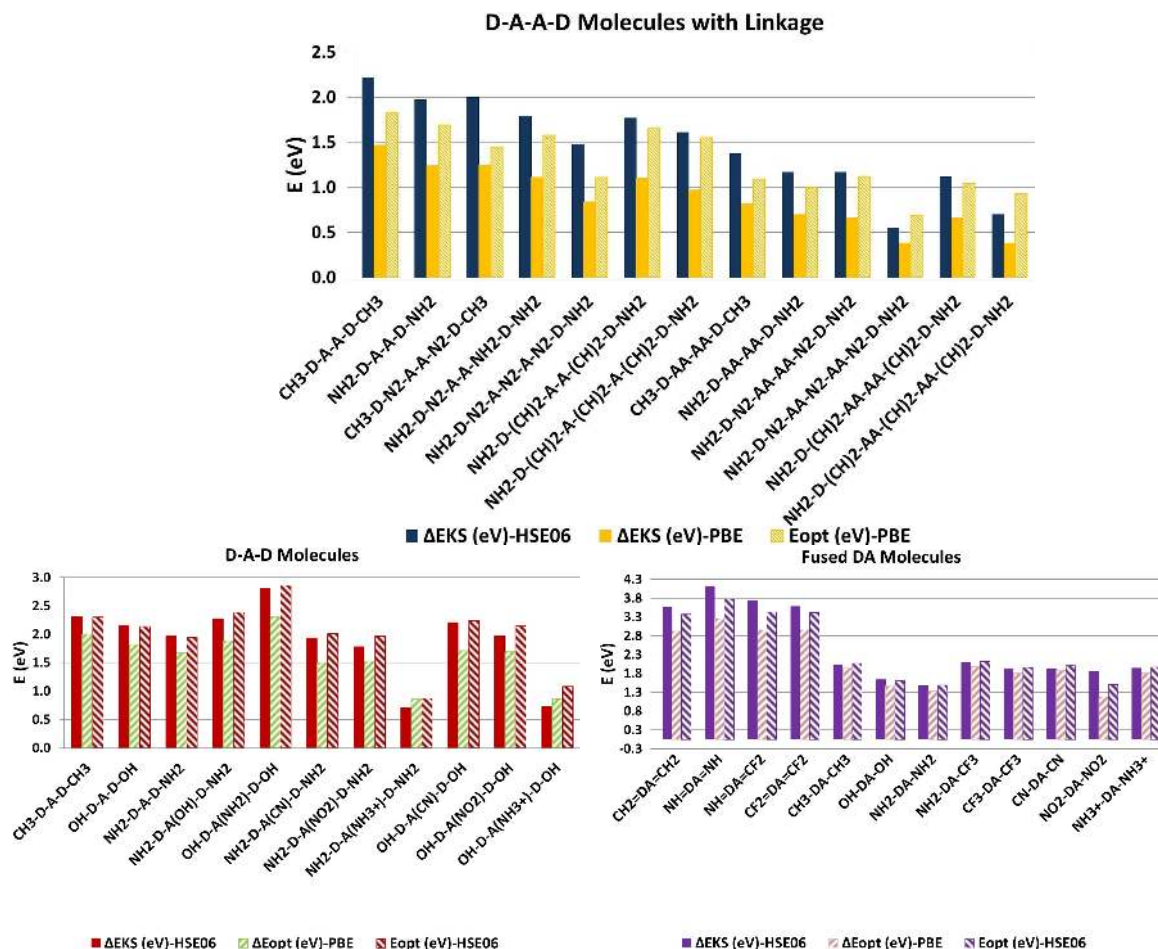


Figure 11: Bar diagram depicting comparison between DFT computed Kohn-Sham HOMO-LUMO energy gap and TDDFT computed optical gap for D-A-A-D molecules with linkages, coupled D-A-D molecules with donor and acceptor ends terminated by EDG or/and EAG or/and H, and fused DA molecules terminated by different EDGs or/and EAGs. EDGs are chosen from $-\text{CH}_3$, $-\text{OH}$, and $-\text{NH}_2$ functional groups while either of the $-\text{NO}_2$, $-\text{CN}$, $-\text{CF}_3$, and $-\text{NH}_3^+$ is considered as EAG.

To summarize, a graphical comparison between the DFT computed Kohn-Sham HOMO-LUMO energy gap and the TDDFT calculated optical gap for all the examined molecules, as tabulated in Tables 1, 2, and 3, is depicted in Figure 11. From the bar diagram it is clearly evident that PBE mostly gives lower gap as compared to HSE06 xc-functional. TDDFT though improves the results for PBE but still gives lesser value than HSE06. While, HSE06

Table 3: Energy levels corresponding to HOMO (E_{HOMO}) and LUMO (E_{LUMO}) and respective Kohn-Sham HOMO-LUMO energy gap (ΔE^{KS}) calculated using HSE06 xc-functional, for fused DA molecules with different terminating groups, is given. For comparison, TDDFT computed optical gap with HSE06 (PBE) xc-functional, is also presented. IP, EA, fundamental gap ($E_{fund}=IP-EA$), together with hole and electron reorganization energies (λ_h and λ_e) are also tabulated. These quantities are calculated using HSE06 xc-functional.

Molecule	a (Å)	E_{HOMO} (eV)	E_{LUMO} (eV)	ΔE^{KS} (eV)	E_{opt} (eV)	IP (eV)	EA (eV)	E_{fund} (eV)	λ_e (eV)	λ_h (eV)
Fused DA Molecules										
CH ₂ =DA=CH ₂	3.02	-5.72	-2.20	3.52	3.32 (2.88)	6.61	1.44	5.17	0.1279	0.1511
NH=DA=NH	3.04	-6.87	-2.80	4.07	3.72 (3.21)	8.18	1.71	6.47	0.1143	0.1464
NH=DA=CF ₂	3.01	-6.27	-2.59	3.68	3.38 (2.91)	7.55	1.55	6.00	0.0586	0.0881
CF ₂ =DA=CF ₂	2.98	-5.82	-2.29	3.53	3.36 (2.91)	7.01	1.34	5.66	0.1066	0.2645
CH ₃ -DA-CH ₃	2.92	-6.21	-4.23	1.97	2.02 (1.89)	7.17	3.33	3.85	0.2589	0.1363
OH-DA-OH	2.91	-4.60	-3.01	1.59	1.56 (1.41)	5.92	1.82	4.10	0.1850	0.2139
NH ₂ -DA-NH ₂	2.95	-4.10	-2.66	1.43	1.44 (1.29)	5.35	1.62	3.72	0.1843	0.5399
NH ₂ -DA-CF ₃	2.94	-5.01	-3.12	1.89	1.92 (1.77)	6.27	1.94	4.33	0.2855	0.1957
CF ₃ -DA-CF ₃	2.91	-5.92	-3.85	2.06	2.07 (1.94)	7.24	2.61	4.63	0.3189	0.1480
CN-DA-CN	2.91	-6.24	-4.36	1.88	1.96 (1.84)	7.44	3.20	4.24	0.15031	0.0045
NO ₂ -DA-NO ₂	2.86	-6.36	-4.50	1.86	1.91 (1.77)	7.62	3.36	4.26	0.5285	0.1621
NH ₃ ⁺ -(DA) ⁻² -NH ₃ ⁺	2.80	-2.83	-1.03	1.80	1.45 (1.13)	4.00	1.09	2.91	0.0476	0.3236

computed HOMO-LUMO energy gap and optical gap are very much in agreement with each other. Also, one can notice that by choosing molecules under considered schemes, the gap can be engineered over a wide range of energy, which varies between 0.7 – 3.7 eV.

CONCLUSIONS

In present work, we modeled three different rationally designed configurations of D-A based molecules and investigated their structural, electronic, and optical properties. These three configurations are designed by: (i) introducing a π -conjugated linkage unit between D-A and A-A units of the D-A-A-D molecules in order to vary the steric hindrance between the moieties, (ii) terminating donor and acceptor moieties by various electron donating and accepting functional groups, to change the strength of the donor and acceptor moieties, and (iii) fusing the donor and acceptor moieties, to increase the rigidity in the molecule. Our study reveals that all three designing schemes work well in engineering the electronic and optical gap of the D-A based molecules. Addition of π -conjugated linkage unit reduces the steric hindrance between the A-A units by enhancing the $\pi - \pi$ interaction, which eventually helps in reducing the HOMO-LUMO energy gap of the D-A-A-D based molecules. On the other hand, terminating the ends of the coupled D-A-D or D-A-A-D molecules by different EDGs and EAGs destabilizes the HOMO and LUMO energy levels, respectively, due to increase in the strength of the donor and acceptor moieties through resonance or inductive effects imposed by EDGs and EAGs. The destabilization of the HOMO and LUMO energy levels result into variation in the electronic and optical gap, as per the strength of the EDG and EAG, and the location where they are attached. Next, our study demonstrates that fusing of donor and acceptor moieties also helps in modulating the opto-electronic properties as due to rigidity of the fused molecule, the overlapping between $\pi - \pi$ interaction increases, which leads to the reduction in the HOMO-LUMO energy gap and the optical gap. The properties of these molecules can further be tuned by terminating the ends of

the base molecule by different EDGs or/and EAGs. Overall, our results reveal that using aforementioned schemes the HOMO-LUMO gap and the optical gap can be tailored over a wide range from $\sim 0.7-3.7$ eV, that covers the light spectrum from infrared to visible to near ultraviolet region. Moreover, our study also elucidates the exceptional behavior of molecules having $-\text{NH}_3^+$ as EAG. Due to strong -I effect, $-\text{NH}_3^+$ polarizes the molecule, that increases the HOMO and LUMO energy levels and gives noticeably lower HOMO-LUMO energy gap. Furthermore, on examining the reorganization energy of the molecules we predict them to exhibit high charge carrier mobility, with the presence of ambipolar characteristics in few of the investigated molecules. Additionally, most of the investigated molecules are predicted to be air-stable, making them suitable candidate for device application. This detailed study not only provides promising materials for the application in opto-electronic devices like OFETs, OLEDs, and OPVs but also facilitates a pathway to design molecules with desired properties.

Acknowledgments This work was initiated in a project carried out at Shiv Nadar University under the Opportunities for Undergraduate Research (OUR) scheme. Authors are thankful to the concerned authorities to make this grant available. P.J. would also like to acknowledge the financial support provided by Grant No. SR/FTP/PS-052/2012 from Department of Science and Technology (DST), Government of India. The high performance computing facility and the workstations available at the School of Natural Sciences, Shiv Nadar University, were used to perform all calculations.

References

- (1) Sonar, P.; Singh, S. P.; Leclere, P.; Surin, M.; Lazzaroni, R.; Lin, T. T.; Dodabalapur, A.; Sellinger, A. *J. Mater. Chem.* **2009**, *19*, 3228–3237.
- (2) Sonar, P.; Singh, S. P.; Sudhakar, S.; Dodabalapur, A.; Sellinger, A. *Chem. Mater.* **2008**, *20*, 3184–3190.
- (3) Polander et. al., L.-. E. *J. Phys. Chem. C* **2011**, *115*, 23149–23163.

- (4) Cheng, Y.-J.; Yang, S.-H.; Hsu, C.-S. *Chem. Rev.* **2009**, *109*, 5868–5923.
- (5) Pandey, L.; Risko, C.; Norton, J. E.; Bredas, J.-L. *Macromolecules* **2012**, *45*, 6405–6414.
- (6) Li, J.-C.; Kim, S.-J.; Lee, S.-H.; Lee, Y.-S.; Zong, K.; Yu, S.-C. *Macromolecular Research* **2009**, *17*, 356–360.
- (7) Li, J.-C.; Meng, Q. B.; Kim, J.-S.; Lee, Y.-S. *Bull. Korean Chem. Soc.* **2009**, *30*, 951–954.
- (8) Bundgaard, E.; Krebs, F. C. *Macromolecules* **2006**, *39*, 2823–2831.
- (9) Wykes, M.; Begona, M.-M.; Gierschner, J. *Frontiers in Chem.: Theo. and Comp. Chem.* **1993**, *1*, 35.
- (10) Gibson, G. L.; McCormick, T. M.; Seferos, S. S. *J. Am. Chem. Soc.* **2012**, *134*, 539–547.
- (11) Cheng, Y.-J.; Chen, C.-H.; Ho, Y.-J.; Chang, S.-W.; Witek, H. A.; C.-S., H. *Org. Lett.* **2011**, *13*, 5484–5487.
- (12) Cheng, Y.-J.; Ho, Y.-J.; Chen, C.-H.; Kao, W.-S.; Wu, C.-E.; Hsu, S.-L.; C.-S., H. *Macromolecules* **2012**, *45*, 2690–2698.
- (13) Kato, S.-I.; Furuya, T.; Kobayashi, A.; Nitani, M.; Ie, Y.; Aso, Y.; Yoshihara, T.; Tobita, S.; Nakamura, Y. *J. Org. Chem.* **2012**, *77*, 7595–7606.
- (14) Kresse, G.; Furthmuller, J. *Phys. Rev. B* **1996**, *54*, 11169–11186.
- (15) Kresse, G.; Furthmuller, J. *Computational Materials Science* **1996**, *6*, 15–50.
- (16) Kresse, G.; Joubert, D. *Phys. Rev. B* **1999**, *59*, 1758–1775.
- (17) Heyd, J.; Scuseria, G. E.; Ernzerhof, M. *J. Chem. Phys.* **2003**, *118*, 8207.
- (18) Heyd, J.; Scuseria, G. E.; Ernzerhof, M. *J. Chem. Phys.* **2006**, *124*, 219906.

- (19) Paier, J.; Marsman, M.; Hummer, K.; Kresse, I. C., G. Gerber; Angyan, J. G. *J. Chem. Phys.* **2006**, *124*, 154709.
- (20) Paier, J.; Marsman, M.; Hummer, K.; Kresse, I. C., G. Gerber; Angyan, J. G. *J. Chem. Phys.* **2006**, *124*, 154709.
- (21) Perdew, J. P.; Burke, K.; Ernzerhof, M. *Phys. Rev. Lett.* **1996**, *77*, 3865–3868.
- (22) Wang, L.; Nan, G.; Yang, X.; Peng, Q.; Shuai, Z. *Chem. Soc. Rev.* **2010**, *39*, 423–434.
- (23) Nan, G.; Shi, Q.; Shuai, Z.; Li, Z. *Phys. Chem. Chem. Phys.* **2011**, *13*, 9736–9746.
- (24) Giannozzi *et al.*, *P. J. Phys.:Condens. Matter* **2009**, *21*, 395502.
- (25) Malcioglu, O. B.; Gebauer, R.; Rocca, D.; Baroni, S. *Comp. Phys. Comm.* **2011**, *182*, 1744–1754.
- (26) Ge, X.; Binnie, S. J.; Rocca, D.; Gebauer, R.; Baroni, S. *Comp. Phys. Comm.* **2014**, *185*, 2080–2089.
- (27) Runge, E.; Gross, E. K. U. *Phys. Rev. Lett.* **1984**, *52*, 997–1000.
- (28) Marques, M. A. L.; Ullrich, C. A.; Nogueira, F.; Rubio, A.; Burke, K.; Gross, E. K. U. *Springer-Verlag, Berlin, Heidelberg* **2006**,
- (29) Johari, P.; Singh, S. P. *J. Phys. Chem. C* **2015**, *119*, 14890–14899.
- (30) Bredas, J.-L. *Mater. Horiz.* **2014**, *1*, 17–19.
- (31) Kuemmel, S.; Kronik, L. *Rev. Mod. Phys.* **2008**, *80*, 3–60.
- (32) Knupper, M. *Appl. Phys. A* **2003**, *77*, 623–626.
- (33) Hummer, K.; Ambrosch-Draxl, C. *Phys. Rev. B* **2005**, *71*, 081202(R).
- (34) Deng, W.-Q.; Goddard III, W. A. *J. Phys. Chem. B* **2004**, *108*, 8614–8621.

- (35) Sokolov *et al.*, A. N. *Nature Comm.* **2011**, *2*, 437.
- (36) Obayes, H. R.; Alwan, G. H.; Al-Amiery, A. A.; Kadhum, A. A. H.; Mohamad, A. B. *Journal of Nanomaterials* **2013**, *2013*, 451920.